Investigating the composition of resveratrol-induced stress granules

A Major Qualifying Project

Submitted to the Faculty of

Worcester Polytechnic Institute

in partial fulfillment of the requirements for the

Degree in Bachelor of Science

in Biology and Biotechnology

By

_____

Sarah Jones

_____

Kathryn Kenney

_____

Abigail O'Connor

Date: 4/27/22

Project Advisors:

_____

Professor Natalie Farny

_____

Professor Lou Roberts

Abstract

Stress granules are RNA- and protein-containing cytoplasmic aggregates that form in response to stress. Cells may have different compositions of stress granules depending upon the type of stress. Previous research has identified proteins including RACK1, RPS3, RPS6, eIF3a, eIF4E, and TRAF2 in arsenite-formed stress granules, which appear to have an anti-apoptotic function. However, these factors are often absent from pro-apoptotic forms of stress granules. Acute high dose exposure to the stilbene compound resveratrol was recently shown to cause stress granules, but the proteins comprising the resveratrol stress granules remained unknown. Therefore we aimed to determine the composition of resveratrol-induced stress granules. U2OS cells were treated with resveratrol, ethanol (a negative control), and arsenite (a positive control), to observe stress granule formation. RACK1, RPS3, RPS6, eIF3a, eIF4E and TRAF2 were detected with antibodies for colocalization to stress granules with the stress granule marker protein G3BP1, using fluorescence microscopy. From this experiment it was found that resveratrol-induced stress granules had G3BP1 colocalization with RACK1, RPS3, RPS6, eIF3a, eIF4E and TRAF2 suggesting that their function is likely anti-apoptotic and similar to arsenite-induced stress granules.

Acknowledgments

We would like to thank our advisors *Natalie Farny and Lou Roberts* for giving us unconditional support throughout our project. Their shared knowledge and experience drove us to perform these experiments and learn as much as we could in our time here. Without them leading us, we would not be where we are today.

We would also like to thank the *WPI Biology and Biotechnology* department for the lab space and materials. We are very thankful to have such a core faculty to have taught us everything we know and for preparing us for what comes next.

Table of Contents

Introduction

When cells are subjected to stressful extreme environments, including extreme temperature, and exposure to toxins, there is a cellular stress response to either repair the damage from the stressor on the cell or terminate the cell. This protective or destructive response is dependent on the severity and duration of the stressor (Fulda et al., 2010). The cellular stress response is initiated when the strain of the stressor deforms/damages proteins, DNA, and macromolecules of the cell (Kültz, 2005). In efforts of maintaining homeostasis within the cell, protective mechanisms counteract the stressor to promote the survival of the cell. This stress response is also referred to as the cellular homeostasis response (Kültz, 2005). In other cases, the cell's defense mechanisms are unable to overcome the stressor deeming the cell 'unfit', initiating programmed cell death (Fulda et al., 2010; Kültz, 2005). As part of this defensive cellular stress response, stress granules (SGs) are formed within the cells. SGs are cytoplasmic aggregates of mRNA translation pre-initiation proteins (Protter et al., 2016). The formation of SGs is typically viewed as a protective response to conserve translational resources to avoid apoptosis and death (Arimoto et al., 2008). SG formation pathways are specific to the causative stress although many form as a downstream effect of the activation of the integrated stress response (Arimoto et al., 2008). The study of SGs is crucial in understanding tumor formation and viral infections (Anderson et al., 2015).

Apoptosis, or programmed cell death, is defined by the morphology of distinct cellular characteristics based on energy-dependent biochemical mechanisms (Elmore et al. 2007). These cellular changes include cell shrinkage and dense cytoplasm with tightly packed organelles (Elmore et al. 2007). Tightly packed organelles are also known as apoptotic bodies and result in budding, which is phagocytosis of the bodies by macrophages. Cells naturally die over time and apoptosis is an important part of maintaining homeostasis (Elmore et al. 2007). These processes of cell death are coordinated by energy-dependent biochemical mechanisms (Elmore et al. 2007). Some mechanisms that have been identified include execution pathways, composed of extrinsic, intrinsic, and granzyme B pathways, which initiate the cascade of cellular stimuli leading to cell death (Elmore et al. 2007). The complex cascade of events is caused by the activation of cysteine proteases or caspases. Once cleavage of caspases, specifically caspase-3, is initiated there is a degradation of nuclear and cytoskeletal proteins. Then, the formation of apoptotic bodies (ApoBDs) occurs through the activation of endonuclease CAD which degrades DNA inside the

nuclei and causes chromatin condensation (Elmore et al. 2007). When apoptosis is not properly regulated in the body, homeostasis and other crucial bodily functions are compromised causing havoc. If extreme pro-apoptosis or anti-apoptosis occurs, humans encounter conditions like autoimmune disorders and cancers, respectively. Regarding SGs, they are known to inhibit apoptosis which also leads to chemotherapeutic resistance, allowing SGs to form and avoid the chemotherapy.

The receptor for activated C kinase 1 (RACK1) is a scaffolding protein that has a seven-blade β-propeller structure that facilitates protein binding (Faux and Scott, 1996). It utilizes inputs from signaling pathways for several cellular activities such as protein synthesis, transcription, protein shuffling, and cell proliferation (Adams, 2011). RACK1 is sequestered from the cytoplasm and into cytoplasmic stress granules in cells under stress by hypoxia, insufficient oxygen supply, or heat shock (Adams, 2011). RACK1 is a crucial component of SGs in cells as it inhibits the activation of mitogen-activated protein kinase (MAPK) pathways, which if activated, cause an apoptotic response in cells under stress (Adams, 2011). Specifically, RACK1 suppresses the activation of methylthioribose kinase 1 (MTK1) inhibiting the signaling required for the apoptosis causing the MTK1-stress-activated protein kinase (SAPK) pathway (Takekawa, Mutsuhiro, et al., 1997). RACK1 is essential for the survival of SG-forming cells, allowing SGs to limit stress-induced cellular damage (Arimoto et al., 2008). Amrito et al. (2008) shows that in type 1 stress responses, RACK1 is sequestered into SGs, but in type 2 stress responses RACK1 is not sequestered allowing it to bind and activate MTK1 MAPKKK. The composition of SGs under most stress conditions remains unknown, but RACK1 is known to play an important role in the formation of type 1 stress granules.

Tumor necrosis factor receptor-associated factor 2 (TRAF2) is an adaptor protein that is transcribed in nearly every tissue in the body (Jiang et al., 2018). Commonly TRAF2 is a target of tumor-derived and pro-inflammatory factors and is critical for the regulation of cell survival and apoptosis (Jiang et al., 2018). Under heat stress, TRAF2 is sequestered into stress granules, thought to be through a protein-protein interaction with eukaryotic translation initiation factor 4 gamma 1 (eIF4G1) (Kim et al., 2005). This addition of TRAF2 to the SGs blocks various TRAF2-mediated signaling processes, including tumor necrosis factor (TNF) signaling (Kim et al., 2005). The inhibition of these processes downregulates the activation of nuclear factor-kB (NF-kB), which is a key factor in the inflammatory response (Kim et al., 2005). In blocking the

pro-inflammatory positive feedback loop, apoptosis due to inflammation can be avoided, promoting cell survival.

The eukaryotic initiation factor (eIF) proteins are responsible for the regulation of translation initiation. eIF protein complex, comprising several subunits, also functions to stabilize the functional ribosomal complex at the start codon (Ali et al., 2017). There are six eIF complexes including, eIF2, eIF3 and eIF4. Through previous research, it is known that the most common mechanism for SG formation is through the phosphorylation of eIF2α (Clemens, 2001). The most complex form of the eIF family is the eIF3 formation, consisting of subunits eIF3a-eIF3m (Dong and Zhang, 2006). Although the mechanisms are still unknown, it is probable that eIF3a expression mediates cell proliferation through cellular stress sensitivities (Dong et al., 2009). Other researchers have pondered eIF3a to be a potential oncogene, inducing oncogenesis through translation regulation (Yin et al., 2018). Of the eIF4 complex, the cap-binding protein eIF4E presents as the rate-limiting subunit responsible for translation initiation through mRNA recruitment. Therefore, enhanced expression of eIF4E has been linked to tumorigenesis and the regulation of tumor formation (Bitterman and Polunovsky, 2015; Zimmer et al., 2000). When the cell is provoked with extracellular stressors, eIF4E undergoes phosphorylation leading to unregulated translation and proliferation with inhibited apoptosis (Bhat et al., 2015). With both eIF3a and eIF4E assumed to be tumerogenic, these proteins continue to be researched for use in cancer therapies.

Ribosomal proteins, RPs, have been discovered to play unique roles beyond their ribosome and protein synthesis properties. For example, RPS3 has DNA repair functions whereas RPS6 has developmental regulation functions (Wool, 1996). RPS3 protein expression was also seen to induce apoptosis, implicating that RPS3 plays a role in cell fate determination (Jang et al., 2003). A more widely researched protein RPS6 gained attention for its phosphorylation properties. (Meyuhas, 2008). Further research has found RPS6 a possible connection between the protein and the target of rapamycin (TOR) kinase pathway which is responsible for translation, rRNA transcription, and ribosomal protein synthesis (Kim et al., 2014). More research needs to be performed regarding RPs to fully understand complexes and pathways involved in their specialized functions regarding SG colocalization.

Resveratrol (Rsv), or 3,4′,5-trihydroxy-trans-stilbene, is a polyphenolic phytoalexin compound associated with beneficial effects in heart disease prevention, aging prevention, and

anti-inflammatory effects. The structure of Rsv is two aromatic rings connected by a styrene double bond as pictured below in Figure 1 (Pervaiz & Holme, 2009).

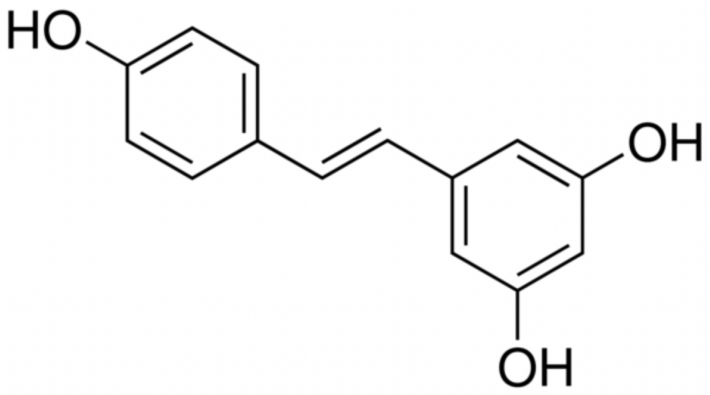

Figure 1. Structure of Resveratrol

Rsv is naturally found in red wine and was hypothesized to contribute to the "French Paradox," or the phenomenon that French people have lower cardiovascular disease despite having a high-fat and high-cholesterol diet (Richard, 1987). Today, Rsv is a new focus for the treatment of human diseases and the prevention of tumors (Szekeres et al., 2010). Rsv is known to cause SGs in cells such as U2OS, but their pathways and composition are unknown (Amen et al., 2021).

In the last two decades, Rsv has been researched for its apoptotic tendencies. Several studies have shown promising results on how Rsv induces apoptosis in cancer cell lines. Rsv has been shown to activate and nuclear translocate MAPK and increase the cellular abundance of protein P53, an oncogene suppressor (Shih et al., 2002). Rsv has been known to induce apoptosis in various cancer cell lines, similar to how cancer chemotherapy drugs induce P53-dependent apoptosis to damage the DNA (Elmore et al., 2002). Along with its apoptotic tendencies in cell lines such as U2OS, Rsv also induces SG formation. Unlike the similar SG induced by stressor arsenite (Ars), Rsv induced SGs are less pronounced and smaller in size. There is also a different clearance mechanism between Ars and Rsv induced SGs, with Rsv SGs having rapid clearance kinetics (Amen et al., 2021). This means that with the removal of the stressor, the SGs disappear and are reversed.

The apoptotic tendencies of Rsv-induced SGs are unknown. SGs can be either pro-apoptotic (type 2) or anti-apoptotic (type 1) depending on their composition, which is related

to the stress that causes them. Since the composition of Rsv SGs remains unknown, in this project we worked to examine the protein composition of Rsv induced SGs. We will be looking specifically to see if they contain pro-apoptotic proteins colocalized at the SG such as RACK1 and TRAF2. With data from previous studies suggesting the similarity in composition of Ars-induced SGs with Rsv-induced SGs, we plan to further investigate whether Rsv SGs contain known components of type 1 SGs including RPS3, RSP6, eIF3a, and eIF4E. While there is evidence of these proteins in Ars-induced SGs, there is a lack of experimental research on Rsv-induced SGs. It is hypothesized that these proteins are in Rsv-induced SGs due to the similarities between Ars- and Rsv-induced SGs. Therefore, the goal of this research is to investigate the composition of Rsv-induced SGs and determine if there are further similarities between the Ars- and Rsv-induced SGs.

Materials and Methods

Cell Line Maintenance

The cell line U2OS (wild-type) was used to investigate the SG protein composition. U2OS is a *Homo sapiens* osteosarcoma cell line derived from the epithelial tissue of bone. This cancer cell line has adherent growth properties (ATCC, 2022). The U2OS cells were maintained in a 37°C incubator in Dulbecco's Modified Eagle Medium (DMEM) with 10% Fetal Bovine Serum (FBS) and 1% penicillin/streptomycin (PS), termed 'DMEM+'. The cells were checked under the inverted microscope every 2-3 days and split depending on the confluency of cells in the flask.

Drug Treatment

18mm round glass coverslips were placed at the bottom of each well in a 12-well plate. 1mL of medium with a concentration of 3.6 x 10^6 /mL wild-type U2OS cells was placed in each of the 12 wells and incubated for 24-48 hours to allow the cells to adhere to the coverslips. After examining the plate under the inverted microscope, 500 µL were removed from each well and added to tubes of the treatment. The treatment setup can be seen in Figure 1 below, with Ars as the positive control and ethanol as the negative control. After incubation, media was removed from the wells and washed with 1x PBS, then removed. The cells were fixed with 4% paraformaldehyde/phosphate buffer saline (PF/PBS), with methanol to permeabilize the U2OS cells, and Hoechst 33325 DNA stain with a 1000x concentration was added, allowing the plate to shake between treatments. Wells were again washed with 1x PBS to maintain cells until the next treatment.

Antibody Staining

Cell antibody staining began with removing 1x PBS from the wells of the 12-well plate and replaced with 5% BSA/ PBS blocking solution, and left to incubate at room temperature.

To prepare for *primary antibody staining*, 3 mL of 5% BSA/PBS was added to 4 tubes, one for each of the primary antibodies - RACK1, TRAF2, eIF3, and RPS3 - used to detect the presence of the four proteins. The specific antibodies used to detect proteins can be found in Table 1 with their respective concentrations indicated. Primary antibodies were added to the corresponding tube as follows: 1:1000 rb-α-G3BP1 in all wells; column 1 wells- 1:2000

ms-α-RACK; column 2 wells - 1:1000 ms-α-TRAF2; column 3 wells - 1:1000 ms-α-eIF3; column 4 wells - 1:1000 ms-α-RSP3, then added to the wells as depicted in Figure 2. Primary antibody staining treatment was left to incubate at room temperature for 60 minutes.

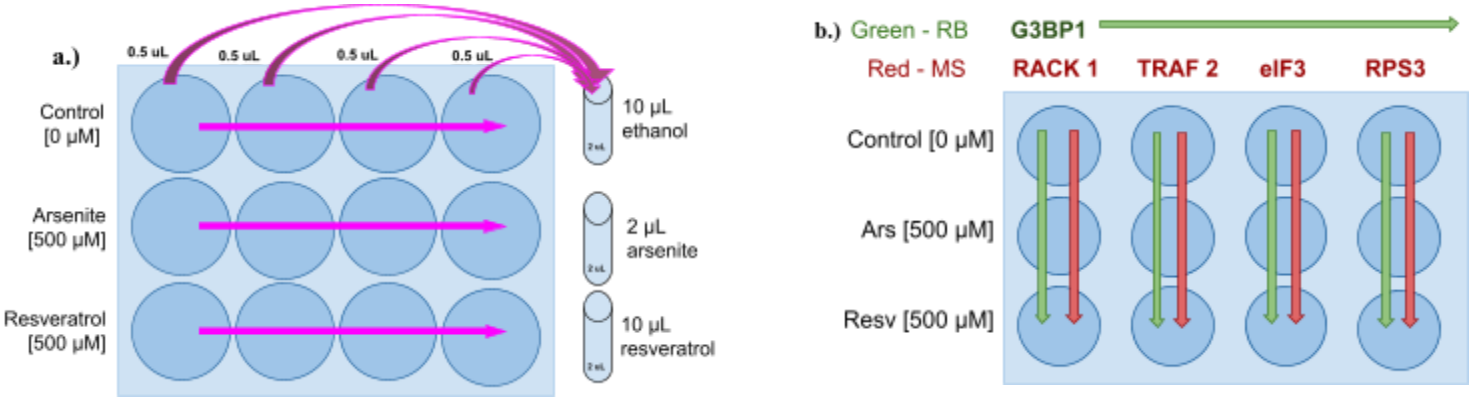

Figure 2. 12-Well Plate Design and Treatment

Following three 1xPBS washes in preparation for secondary antibody staining, a conical tube was prepared with 12 mL of 5% BSA/PBS. Secondary antibodies: 12 µL of anti-rb-A488 (1:1000), 12 µL of anti-ms-A594 (1:1000), and 12 µL of Hoechst 33325 DNA stains (1:1000) were added to the tube. 0.5 mL of secondary antibody stains were added to all 12 wells. The secondary antibody stains were removed and washed three more times with 1xPBS.

Table 1. Antibodies used in this study

Antibody	Ratios	Manufacturer	Product #
rabbit(rb)-anti(α)-G3BP1	1:1000	Proteintech	13057-2-AP
mouse (ms)-α-G3BP1	1:1000	Proteintech	66486-1-Ig
ms-α-RACK1	1:2000	Proteintech	66940-1-Ig
ms-α-TRAF2	1:1000	Proteintech	67315-1-Ig
rb-α-TRAF2	1:1000	ABclonal	A0962
ms-α-eIF3	1:1000	Proteintech	67713-1-Ig

rb-α-eIF3a	1:1000	ABclonal	A0573
rb-α-eIF4E	1:1000	ABclonal	A6085
ms-α-RSP3	1:1000	Proteintech	66046-1-Ig
rb-α-RPS6	1:1000	ABclonal	A6058
α-rb- IgG Alexa Fluor 488 (green) stain	1:1000	Cell Signaling Technology	4412S
α-ms- IgG Alexa Fluor 488 (green) stain	1:1000	Cell Signaling Technology	4408S
α-ms- IgG Alexa Fluor 594 (red) stain	1:1000	Cell Signaling Technology	8890S
α-rb- IgG Alexa Fluor 594 (red) stain	1:1000	Cell Signaling Technology	8889S
Hoechst 33325 nuclear (blue) stain	1:1000	Thermo Scientific	62249

The coverslips from each well were plated on microscope slides using vinol mounting medium with cell side face down and labeled with drug treatment and antibody stain to prepare for fluorescence microscopy.

Microscopy

Using the Zeiss Light Microscope Axio Observer A1, with a total magnification of 400x, cells were located using the eyepiece and brought into focus. The microscope view was shifted to the camera and the program SPOT basic was used to capture pictures of the cells. The green fluorescent filter was used to capture stress granules in the cells at an exposure of 1000ms. The red fluorescent filter was used to capture antibody stain presence in the cells at an exposure of 6000ms. Both fluorescent channel pictures were taken of the same coverslip cell field. The images were then saved to be used for fluorescence intensity quantification of the stained antibodies co-localized at the SGs.

SG Quantification

Each blinded slide was viewed under the green fluorescent filter to view the GFP-tagged antibodies within the cells. At least 250 cells were counted across different fields of the coverslips. The cells were counted by each researcher and the numbers of SG positive cells and SG negative cells were recorded. The data from the same slides were compared among researchers to ensure SGs counts were consistent among all members (Appendix A). This practice quantification was performed several times until there was consistency among the group.

SG Protein Co-Localization via Stained Antibody Analysis

Using the program Image J from NIH (*https://imagej.nih.gov/ij/*), the green and red fluorescent filter images were uploaded per coverslip cell field, (example: image E1.2 G(reen)-Resv-RACK1 and image E1.2 R(ed)-Resv-RACK1). The two images were overlaid using the *stack* feature. On the green fluorescent image, a line was drawn through SGs of a cell then analyzed using the *plot profile* feature to quantify the green fluorescence values of the SG. Switching over to the stacked red fluorescent image, maintaining the line position, the line was analyzed again using the plot profile feature to quantify the red fluorescence values over the location of the SG. The plot profile values were uploaded to Microsoft Excel to plot fluorescence values. The graphs were analyzed for similar fluorescent value peaks at the same distance along with the line position. Three cells per two fields were analyzed using the methods entailed above.

Results

SG Formation

U2OS cells were treated with ethanol (negative control), Ars (positive control), and Rsv in order to determine if Rsv caused SG formation. The formation of SGs in cells treated with Rsv can be seen in Figure 3. Each of the cell treatments were qualitatively analyzed using the fluorescence microscope. The most SGs were seen in the positive control cells treated with Ars, then the cells treated with Rsv, and little to none in ethanol. Once we were able to show that Rsv caused SGs in U2OS cells, the majority of our efforts were used in perfecting the experiment to optimize the results obtained.

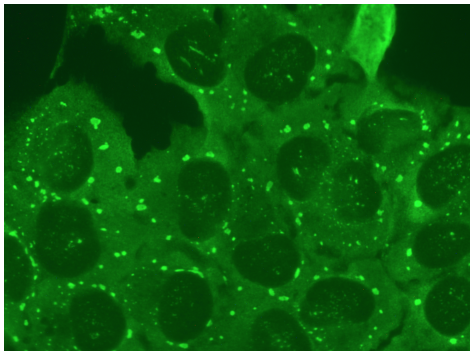

Figure 3. A488 Stained G3BP1 Marking SGs in U2OS Cells

Quantifying SG Formation in Response to Rsv

The first experiment was performed to determine the best concentration of Rsv to use in order to cause SGs as well as practice identifying and counting SGs consistently. Cells were plated in a 12-well plate with 3 treatment concentrations of Rsv. After the experiment, the slides were blinded and SGs counted. The data from this trial (Appendix A) shows two group members having similar SG counts shown in red and blue, while the other had comparably high SG counts. The first attempt counting the SGs showed variation amongst group members which were corrected by clarifying what was considered a positive SG. It was confirmed by this experiment that Rsv produced SGs at 500 mM. This concentration was used for all future experiments.

Optimizing Antibody Concentrations to Determine SG Composition

Antibody staining was used to collect colocalization data on the four proteins RACK1, TRAF2, eIF3, and RPS3. The experiments began using 1:2000 for RACK1 and 1:1000 TRAF2, eIF3, and RPS3 for the primary antibodies. For the secondary antibodies 1:1000 was used for anti-rbA488, anti-ms594 and in addition to 1:1000 Hoechst dye. For each protein one image was taken on the green filter and red filter using SPOT software. From there the images were overlaid in ImageJ and a line was drawn through one or two SGs. A plot of the fluorescence profile was created for both images in the stack. This data was put onto the same graph to compare the fluorescence peaks between G3BP1, indicating SGs, and the protein. Colocalization was determined by correlating peaks in the antibody-stained proteins shown as the red line. Appendix B shows a chart where each slide was assessed on the quality of each staining. Appendix C and D show images of the cells that stained well which for the most part was RACK1 and RPS3. It was hard to tell if the issue was the staining concentrations or the antibodies themselves.

Several experiments were performed in order to gather data for the other four proteins, but challenges were encountered with lack of SG formation for Rsv treated cells and poor antibodies. The new antibodies worked much better allowing for imaging and analysis to be performed even though SGs did not form (Appendix E). It was thought that the Rsv stock had lost efficacy and therefore was no longer inducing the formation of SGs during drug treatment. The stock Rsv was remade for the final trial. Once the Rsv was replaced, SGs formed in the treated cells and data was collected for the remaining proteins eIF3a, eIF4E, RPS3, and RPS6.

RACK1 and TRAF2 were expected to be in Rsv formed SGs, since they are both pro apoptotic proteins that are known to be sequestered into Ars SGs. As hypothesized, the SG marker protein G3BP1 colocalized with both RACK1 and TRAF2. The green lines of the Figure 4 fluorescence graphs show the G3BP1 peaks marking the SGs themselves. To determine colocalization the protein should have peaks in the same location as the SGs, therefore showing that the SG and the protein are in the same location. Both proteins show colocalization, but TRAF2 looks as if it has better colocalization. It is important to note that the significance or amount of colocalization cannot be determined from this data and antibodies cannot be cross compared since they each have different binding affinities.

A.

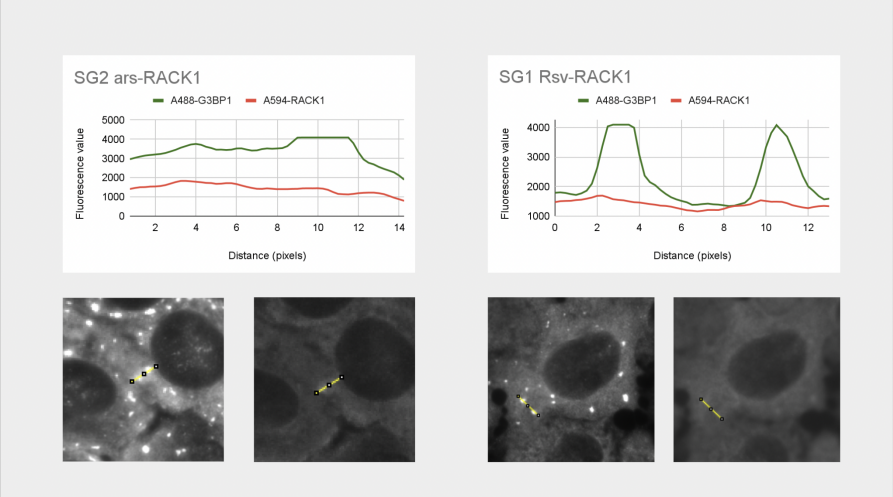

B.

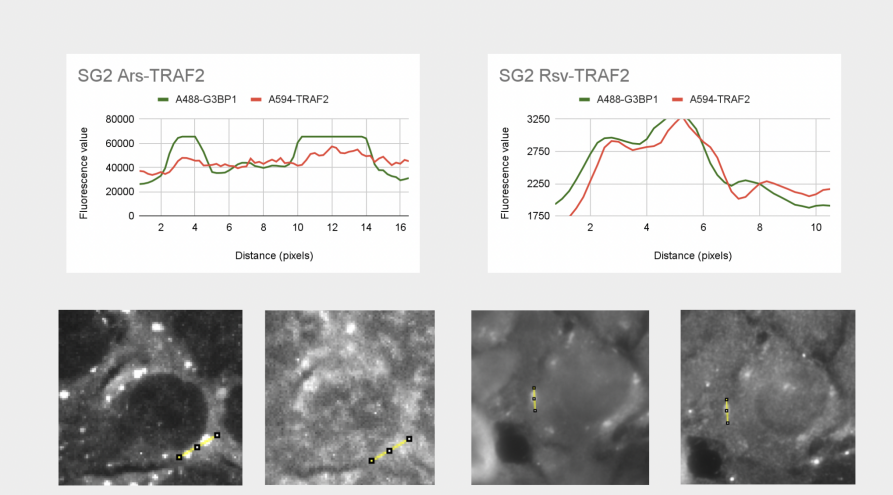

Figure 4. RACK1 and TRAF2 colocalization in Rsv formed SGs

Fluorescence microscopy of both Ars (positive control) and Rsv stained with antibodies to detect RACK1 (A) or TRAF2 (B) proteins (red, right panel images) and G3BP1 (green, left panel images). Under each graph are the images from the green and red fluorescent filters with a line drawn through 1-3 SGs, creating the fluorescence data.

The proteins eIF3a and eIF4E were anticipated to have similar results since they are both a part of the translation initiation complex. While these proteins do not appear in the literature for Rsv SGs, there is some data showing that they are found in Ars SGs. The experiments with the new Rsv stock and new antibodies used the same methods as the previous experiments. As seen in Figure 5, the proteins each have clear colocalization in Rsv SGs as each set of peaks

match up between the SG and the protein. This shows that the translation initiation complex plays a role in SG formation and conservation of translational resources.

A.

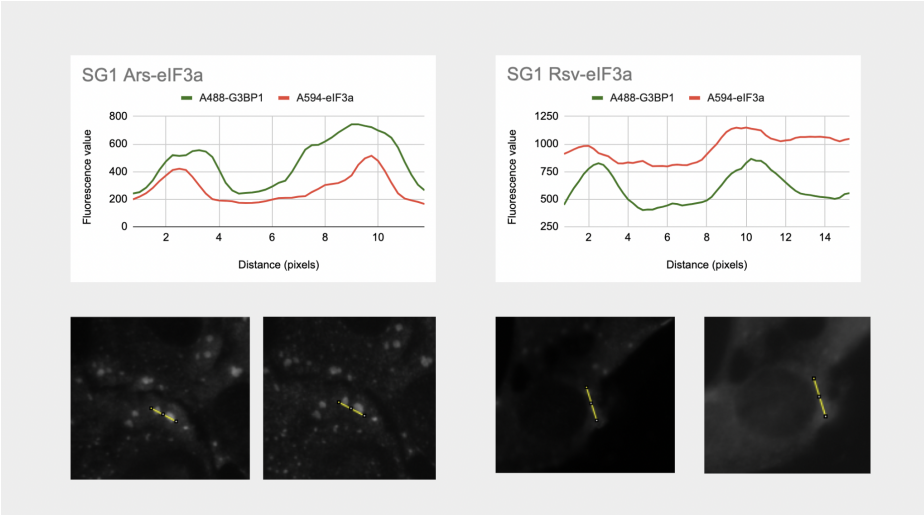

B.

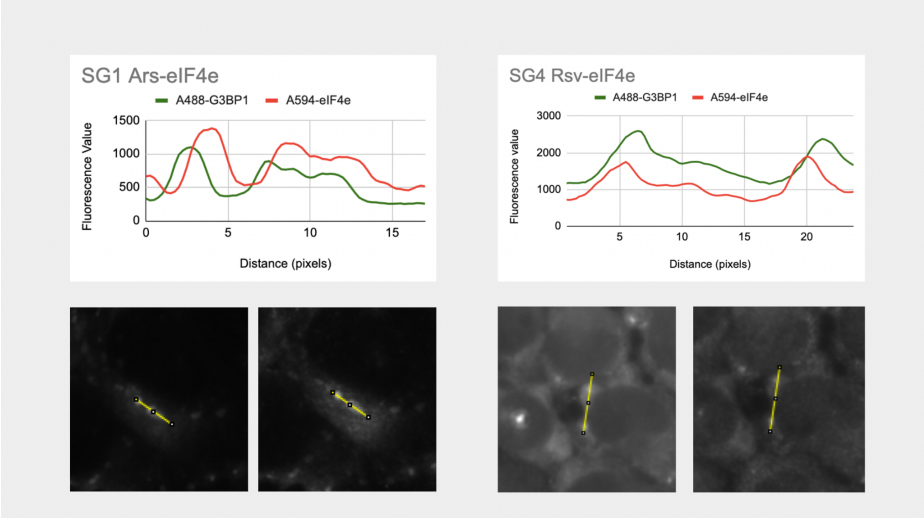

Figure 5. eIF3a and eIF4E colocalization in Rsv formed SGs

Fluorescence microscopy of both Ars (positive control) and Rsv stained with antibodies to detect eIF3a (A) or eIF4E (B) proteins (red, right panel images) and G3BP1 (green, left panel images). Under each graph are the images from the green and red fluorescent filters with a line drawn through 1-3 SGs, creating the fluorescence data.

The proteins RPS3 and RPS6 are similar to eIF3a and eIF4E in that they are not found in the literature for Rsv SGs. They are both members of the small ribosomal subunit and are

sequestered into Ars SGs. The RPS3 graphs in Figure 6 show clear colocalization from the matching peaks between the SG and protein. While the RPS6 graphs are noisy, there are similar peaks between the SG and protein in both the Ars control and the Rsv. This suggests that the ribosomal subunit plays a role in SG formation since these proteins are sequestered into the SGs.

A.

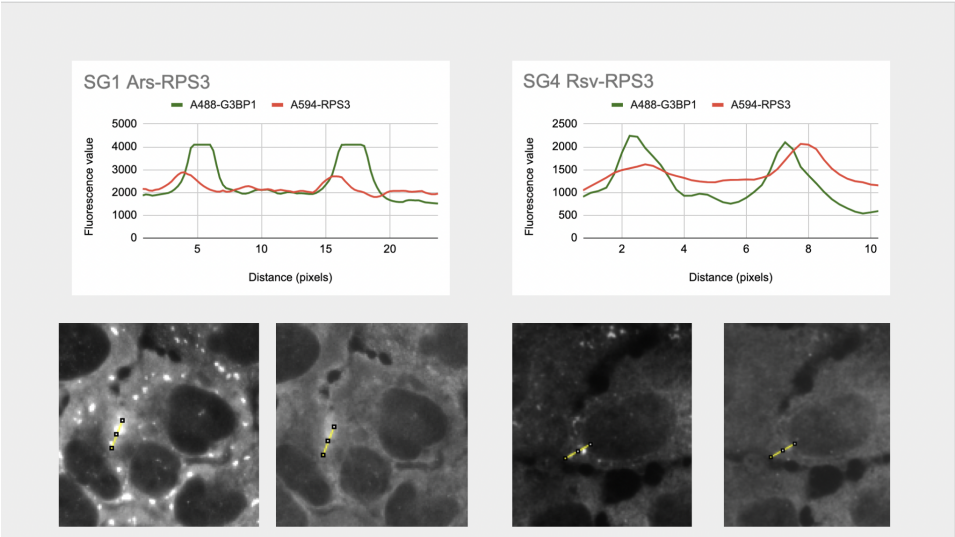

B.

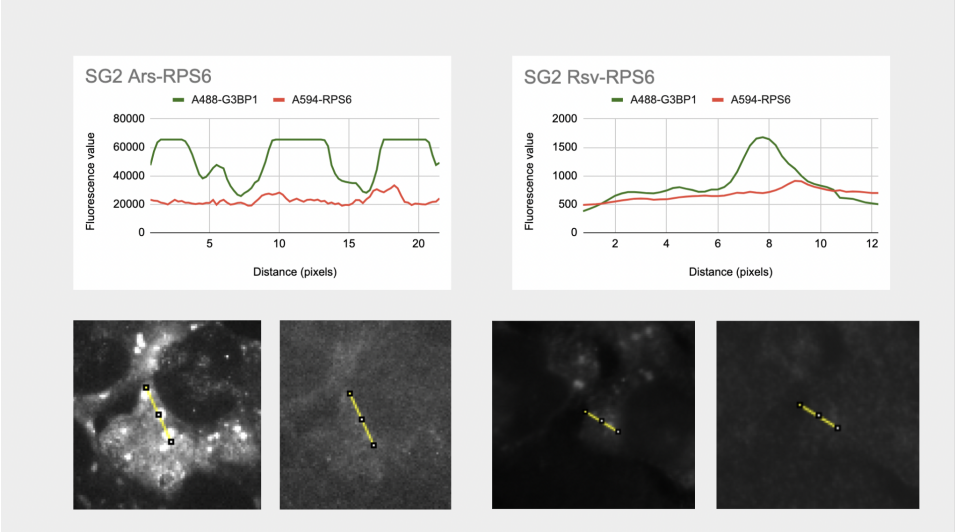

Figure 6. RPS3 and RPS6 colocalization in Rsv formed SGs

Fluorescence microscopy of both Ars (positive control) and Rsv stained with antibodies to detect RPS3 (A) or RPS6 (B) proteins (red, right panel images) and G3BP1 (green, left panel images). Under each graph are the images from the green and red fluorescent filters with a line drawn through 1-3 SGs, creating the fluorescence data.

Discussion

When a cell is placed under stress, the cell responds by forming RNA- and protein-containing cytoplasmic aggregates known as SGs. The composition of these stress granules is dependent on the type of stress placed upon the cells, with our experiment expanding on previous research, identifying the composition of arsenite-induced SGs. It was previously identified that Ars-induced SGs are composed of the proteins RACK1, RPS3, eIF3, and TRAF2, and appear to have anti-apoptotic properties. With recent studies showing SG formation after exposure to the stilbene drug treatment Rsv, our project aimed to determine if RACK1, RPS3, eIF3, TRAF2, and similar proteins compose Rsv-induced SGs.

We show that Rsv induced SGs have G3BP1 colocalization with the proteins RACK1, TRAF2, eIF3a, eIF4E, RPS3 and RPS6. This indicates that the proteins are sequestered into Rsv formed SGs, similarly to the anti-apoptotic Ars induced SGs. It was seen that the peaks of the fluorescence graphs for each protein (red) correlated with the G3BP1 line (green) (Figure 4), meaning the proteins are colocalized in the G3BP1 marked SGs.

TRAF2 had the greatest difference in signal localization within the SG compared to the surrounding cytoplasm. (Figure 4B). This means there is strong colocalization of TRAF2 in Rsv SGs. eIF3a/4E (Figure 5) and RPS3/6 (Figure 6) all show signal localization to the SG that is above the background of the surrounding cytoplasm, though the colocalization represents a small amount of the total protein detected. These data support at least partial colocalization of eIF3a, eIF4E, RPS3 and RPS6 at SGs.

There is a slight discrepancy in the Rsv-RACK1 fluorescence graph (Figure 4A) as the RACK1 line only has very slight peaks corresponding to the G3BP1 line. This is also seen in the Ars-RACK1 graph (Figure 4A) as the RACK1 line follows a similar peak pattern to the G3BP1 line, but the fluorescence values for RACK1 are 1500 below those of G3BP1. This could indicate that the colocalization of RACK1 in Rsv and Ars induced SGs is weaker than what is seen with TRAF2, eIF3, and RPS3. It could also be that the staining antibody for RACK1 is of lesser quality than the others, resulting in lower fluorescence values.

There were challenges throughout the experiment that can be avoided in the future. It was found that the antibody staining for the proteins needs to be high quality in order to stain well enough to observe under the corresponding filter of the Zeiss Light Microscope Axio Observer

A1. The antibodies being used in the initial experiments did not stain well, making it difficult to observe the cells under the red microscope filter for RACK1, TRA2, eIf3a/4e and RPS3/6. It was also found that Rsv stock in solution needs to be replaced monthly to generate stress granules in cells.

Previous research found that Rsv induces SGs at similar concentration to an Ars treatment in human HEK293T cells (Amen et al. 2021). This article also showed that Rsv induces SGs in two other human cell lines: HeLa and U2OS. This information was the foundation for our experimental trials as it was known that using the U2OS cell line would produce Rsv induced SGs.

The localization of TRAF2 and RACK1 to Rsv SGs suggests that Rsv SGs may be anti-apoptotic or cytoprotective under stress conditions. In order to confidently determine whether Rsv SGs are anti-apoptotic, further research needs to be done. Prolonged observation of live Rsv treated cells can be conducted to determine if the cells will undergo apoptosis or not. For anti-apoptotic stress granules, cells that form stress granules should live longer under stress than cells that do not or cannot form stress granules. Co-staining with apoptotic markers such as Annexin V could also be used to identify apoptotic cells in response to Rsv treatment.

These results bring us closer to uncovering the therapeutic utility of Rsv. Our observations that RACK1, TRAF2, eIF3, eIF4E, RPS3 and RPS6 are sequestered into and colocalize in Rsv SGs permit generation of new hypotheses about the function of Rsv SGs. For example, TRAF2 is responsible for blocking the pro-inflammatory positive feedback loop (Jiang et al., 2018). The strong colocalization of TRAF2 in Rsv SGs may suggest potential pro-inflammatory properties of Rsv SGs, though this remains to be determined. Further research on the chemotherapeutic resistance and anticarcinogenic properties of Rsv SGs will provide a clearer picture on how Rsv can be used for disease treatment.

References

Adams, D. R., Ron, D., & Kiely, P. A. (2011). RACK1, A multifaceted scaffolding protein: Structure and function. *Cell Communication and Signaling, 9,* 22. https://doi.org/10.1186/1478-811X-9-22

Ali, M. U., Ur Rahman, M. S., Jia, Z., Jiang, C. (2017) Eukaryotic translation initiation factors and cancer. *Tumour biology : the journal of the International Society for Oncodevelopmental Biology and Medicine, 39(6)*, 1010428317709805. https://doi.org/10.1177/1010428317709805

Amen, T., Guihur, A., Zelent, C., Ursache, R., Wilting, J., & Kaganovich, D. (2021). Resveratrol and related stilbene-derivatives induce Stress Granules with distinct clearance kinetics. *Molecular biology of the cell, 32(21),* ar18. https://doi.org/10.1091/mbc.E21-02-0066

Anderson, P., Kedersha, N., & Ivanov, P. (2015). Stress granules, P-bodies and cancer. *Biochimica et Biophysica Acta*, 1849(7), 861–870. https://doi.org/10.1016/j.bbagrm.2014.11.009

Arimoto, K., Fukuda, H., Imajoh-Ohmi, S., Saito, H., & Takekawa, M. (2008). Formation of stress granules inhibits apoptosis by suppressing stress-responsive MAPK pathways. *Nature Cell Biology*, *10*(11), 1324–1332. https://doi.org/10.1038/ncb1791

ATCC. (2022) *U-2 OS.* Retrieved from: https://www.atcc.org/products/htb-96#detailed-product-information

Benitez, D. A., Pozo-Guisado, E., Alvarez-Barrientos, A., Fernandez-Salguero, P. M., & Castellón, E. A. (2007). Mechanisms Involved in Resveratrol-Induced Apoptosis and Cell Cycle Arrest in Prostate Cancer—Derived Cell Lines. *Journal of Andrology*, 28(2), 282–293. https://doi.org/10.2164/jandrol.106.000968

Bhat, M., Robichaud, N., Hulea, L., Sonenberg, N., Pelletier, J., & Topisirovic, I. (2015). Targeting the translation machinery in cancer. *Nature Reviews Drug Discovery*, 14(4), 261–278. https://doi.org/10.1038/nrd4505

Bitterman, P. B., & Polunovsky, V. A. (2015). eIF4E-mediated translational control of cancer incidence. *Biochimica et Biophysica Acta*, 1849(7), 774–780. https://doi.org/10.1016/j.bbagrm.2014.09.007

Clemens M. J. (2001). Initiation factor eIF2 alpha phosphorylation in stress responses and apoptosis. *Progress in Molecular and Subcellular Biology*, 27, 57–89. https://doi.org/10.1007/978-3-662-09889-9_3

Dong, Z., Liu, Z., Cui, P., Pincheira, R., Yang, Y., Liu, J., & Zhang, J. T. (2009). Role of eIF3a in regulating cell cycle progression. *Experimental Cell Research*, 315(11), 1889–1894. https://doi.org/10.1016/j.yexcr.2009.03.009

Dong, Z., & Zhang, J. T. (2006) Initiation factor eIF3 and regulation of mRNA translation, cell growth, and cancer. *Critical Reviews in Oncology/Hematology*, 59(3), 169–180. https://doi.org/10.1016/j.critrevonc.2006.03.005

Elmore, S. (2007). Apoptosis: A Review of Programmed Cell Death. *Toxicologic Pathology*, 35(4), 495–516. https://doi.org/10.1080/01926230701320337

Faux, Maree C., Scott, John D. (1996) Molecular glue: Kinase anchoring and scaffold proteins. *Cell, 85(1),* 9–12. https://doi.org/10.1016/S0092-8674(00)81075-2.

Fay, M. M., Columbo, D., Cotter, C., Friend, C., Henry, S., Hoppe, M., Karabelas, P., Lamy, C., Lawell, M., Monteith, S., Noyes, C., Salerno, P., Wu, J., Zhang, H. M., Anderson, P. J., Kedersha, N., Ivanov, P., & Farny, N. G. (2021). Bisphenol A promotes stress granule assembly and modulates the integrated stress response. *Biology Open*, *10*(1). https://doi.org/10.1242/bio.057539

Fulda, S., Gorman, A. M., Hori, O., & Samali, A. (2010). Cellular stress responses: cell survival and cell death. *International Journal of Cell Biology, 2010*, 214074. https://doi.org/10.1155/2010/214074

Jang, C. Y., Lee, J. Y., Kim, J. (2004) RpS3, a DNA repair endonuclease and ribosomal protein, is involved in apoptosis. *FEBS Letters, 560(1-3)*, 81–85. https://doi.org/10.1016/S0014-5793(04)00074-2

Jiang, J., Zhang, J., Wu, C., Guo, X., Chen, C., Bao, G., Sun, Y., Chen, J., Xue, P., Xu, G., & Cui, Z. (2018). Up-regulation of TRAF2 inhibits chondrocytes apoptosis in lumbar facet joint osteoarthritis. *Biochemical and Biophysical Research Communications*, *503*(3), 1659–1665. https://doi.org/10.1016/j.bbrc.2018.07.096

Kim, Woo Jae, et al. Sequestration of TRAF2 into stress granules interrupts tumor necrosis factor signaling under stress conditions. *Molecular and Cellular Biology*, *25(6)*, 2450–62. https://doi.org/10.1128/MCB.25.6.2450-2462.2005

Kim, Y. K., Kim, S. Shin, Y. J., Hur, Y. S., Kim, W. Y., Lee, M. S., Cheon, C. I., & Verma, D. P. S. (2014) Ribosomal protein S6, a target of rapamycin, is involved in the regulation of rRNA genes by possible epigenetic changes in *Arabidopsis*. *Plant Bio. 289(7)*, 3901-3912. https://doi.org/10.1074/jbc.M113.515015

Kültz D. (2005). Molecular and evolutionary basis of the cellular stress response. *Annual Review of Physiology, 67*, 225–257. https://doi.org/10.1146/annurev.physiol.67.040403.103635

Losa, G. A. (2003). Resveratrol modulates apoptosis and oxidation in human blood mononuclear cells. *European Journal of Clinical Investigation, 33(9)*, 818–823. https://doi.org/10.1046/j.1365-2362.2003.01219.x

Meyuhas O. (2008). Physiological roles of ribosomal protein S6: one of its kind. *International Review of Cell and Molecular Biology, 268*, 1–37. https://doi.org/10.1016/S1937-6448(08)00801-0

Pervaiz, S., & Holme, A. L. (2009). Resveratrol: Its Biologic Targets and Functional Activity. *Antioxidants & Redox Signaling, 11(11)*, 2851–2897. https://doi.org/10.1089/Ars.2008.2412

Protter, David S. W., and Roy Parker. (2016)Principles and properties of stress granules. *Trends in Cell Biology, 26 (9),* 668–79. https://doi.org/10.1016/j.tcb.2016.05.004.

Richard J. L. (1987). Les facteurs de risque coronarien. Le paradoxe français [Coronary risk factors. The French paradox]. *Archives des Maladies du Coeur et des Vaisseaux*, 80, 17–21.

Shih, A., Davis, F. B., Lin, H.-Y., & Davis, P. J. (2002). Resveratrol Induces Apoptosis in Thyroid Cancer Cell Lines via a MAPK- and p53-Dependent Mechanism. *The Journal of Clinical Endocrinology & Metabolism*, 87(3), 1223–1232. https://doi.org/10.1210/jcem.87.3.8345

Szekeres, T., Fritzer-Szekeres, M., Saiko, P., & Jäger, W. (2010). Resveratrol and Resveratrol Analogues—Structure—Activity Relationship. *Pharmaceutical Research*, *27*(6), 1042–1048. https://doi.org/10.1007/s11095-010-0090-1

Takekawa, Mutsuhiro, et al. (1997)A Human homolog of the yeast Ssk2/Ssk22 MAP kinase kinase kinases, MTK1, mediates stress-induced activation of the P38 and JNK pathways. *The EMBO Journal*, *16 (16)*, 4973–82. https://doi.org/10.1093/emboj/16.16.4973

Treeck, B. V., Protter, D. S. W., Matheny, T., Khong, A., Link, C. D., & Parker, R. (2018). RNA self-assembly contributes to stress granule formation and defining the stress granule transcriptome. *Proceedings of the National Academy of Sciences,* 115(11), 2734–2739. https://doi.org/10.1073/pnas.1800038115

Yin, J. Y., Zhang, J. T., Zhang, W., Zhou, H. H., & Liu, Z. Q. (2018). eIF3a: A new anticancer drug target in the eIF family. *Cancer Letters*, 412, 81–87. https://doi.org/10.1016/j.canlet.2017.09.055

Wool, I.R. (1996). Extratibosomal functions of ribosomal proteins. *Trends in Biochemical Sciences* 21(5), 164-165. https://doi.org/10.1016/S0968-0004(96)20011-8

Zimmer, S. G., DeBenedetti, A., & Graff, J. R. (2000). Translational control of malignancy: the mRNA cap-binding protein, eIF-4E, as a central regulator of tumor formation, growth, invasion and metastasis. *Anticancer Research*, 20(3A), 1343–1351.

Appedencies

A. Stress Granule Formation by Resveratrol and Quantitation

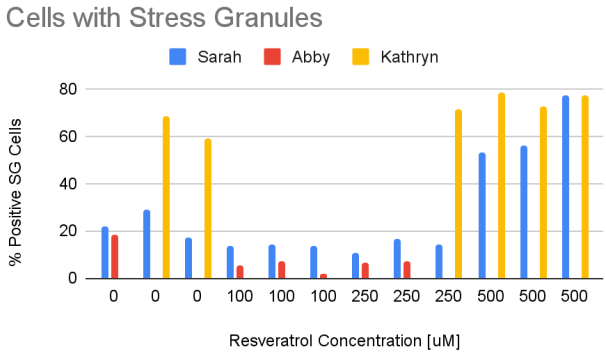

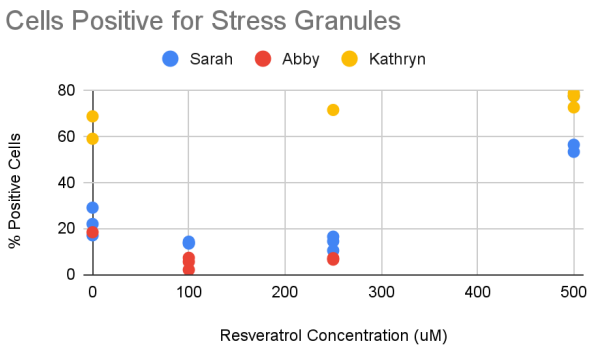

Each researcher counted Resveratrol formed SGs using the same blinded slides. There was variation amongst researchers on the cutoff for what was or was not a stress granule leading to spread data. From this test, it was found that the researchers needed to be more clear with each other to determine SG counts.

B. Problem Solving with Antibody Staining Discrepancies

Experiment 1 — Cell Analysis

Kathryn

Coverslip	Nuclei Stained	Red Staining	SG Staining	Comments
Resv RACK1 1	☑	☑	☑	
Resv TRAF2 1	☑	☐	☐	
Resv TRAF2 2	☐	☐	☐	No cells
Resv RACK1 2	☐	☐	☐	Faint cells
EtOH eIF3	☑	☐	☐	Red/SG smudgey
EtOH RPS3	☑	☑	☑	
Resv RSP3 2	☐	☐	☐	Bad no cells
Resv eIF3 2	☐	☐	☐	Bad no cells
etOH RACK1	☑	☑	☑	faint, but present SG staining
etOH TRAF2	☑	☐	☐	no staining on Red/SG
Ars RACK1	☑	☑	☑	too confluent, faint red staining
Ars TRAF2	☑	☐	☑	
Resv eIF3 1	☑	☐	☐	
Resv RPS3 1	☑	☑	☑	
Ars eIF3	☑	☐	☑	
Ars RPS3	☑	☑	☑	

Sarah

Coverslip	Nuclei Stained	Red Staining	SG Staining	Comments
Resv RACK1 1	☑	☑	☑	
Resv TRAF2 1	☑	☐	☐	
Resv TRAF2 2	☐	☐	☐	no cells
Resv RACK1 2	☐	☐	☐	faint nuclei, cell fragments
EtOH eIF3	☑	☐	☐	faint cells, some red
EtOH RPS3	☑	☑	☐	faint cells
Resv RSP3 2	☐	☐	☐	weird bubble looking things
Resv eIF3 2	☐	☐	☐	absolutely nothing
etOH RACK1	☑	☐	☐	faint cells
etOH TRAF2	☑	☐	☐	faint cells
Ars RACK1	☑	☑	☑	cells too confluent to count, red faint but there
Ars TRAF2	☑	☐	☑	beautiful other than the red
Resv eIF3 1	☑	☑	☑	way too confluent
Resv RPS3 1	☑	☐	☐	blurry
Ars eIF3	☑	☐	☑	cells blurry
Ars RPS3	☑	☑	☑	red and green a little blurry

Abby

Coverslip	Nuclei Stained	Red Staining	SG Staining	Comments
Resv RACK1 1	☑	☑	☑	A++++
Resv TRAF2 1	☑	☐	☐	
Resv TRAF2 2	☐	☐	☐	no cells
Resv RACK1 2	☐	☐	☐	very faint and blurry cells
EtOH eIF3	☑	☐	☐	SG too blurry, red too faint
EtOH RPS3	☑	☑	☑	SG wasn't the best but could distinguish cells enoug
Resv RSP3 2	☐	☐	☐	no cells
Resv eIF3 2	☐	☐	☐	no cells
etOH RACK1	☑	☑	☑	not the best SG
etOH TRAF2	☑	☐	☐	no red/SG
Ars RACK1	☑	☑	☐	SG blobby, cells are not distinct
Ars TRAF2	☑	☐	☑	No red, very confluent
Resv eIF3 1	☑	☑	☐	SG blobby and blurry, red faint but there
Resv RPS3 1	☑	☑	☑	SG slightly blurry but cells are distinct enough, best red so far
Ars eIF3	☑	☐	☑	SG cells blury
Ars RPS3	☑	☑	☑	SG slighlty blurry but not bad, red faint

Trends	
Nuclei Stained	didn't work in some of the resv but its not consistent
Red Staining	worked in RACK1 and RPS3, not the rest
SG Staining	didn't work in any eIF3, most TRAF2, and inconsistent in the rest
Other	a good amount of slides were too confluent or too blurry to count

Experiment 1 | Cell Analysis

Kathryn

Coverslip	Nuclei Stained	Red Staining	SG Positive	SG Negative	Comments
EtOH RACK1	☑	☑	☐	☑	
EtOH TRAF2	☑	☑	☐	☑	very faint red
EtOH eIF3	☑	☐	☐	☑	
EtOH RPS3	☑	☑	☐	☑	
Ars RACK1	☑	☑	☑	☐	Lots of SGs
Ars TRAF2	☑	☐	☑	☐	
Ars eIF3	☑	☑	☑	☐	Faint red, Lots of SGs
Ars RSP3	☑	☑	☑	☐	
Resv eIF3	☑	☑	☑	☐	Faint red
Resv RPS3	☑	☑	☑	☐	Lots of SGs
Resv RACK1	☑	☑	☐	☑	
Resv TRAF2	☑	☐	☐	☑	barely any red

Coverslip	Nuclei Stained	Red Staining	SG Positive	SG Negative	Comments
EtOH RACK1	☑	☑	☐	☑	
EtOH TRAF2	☑	☐	☐	☑	
EtOH eIF3	☑	☑	☑	☐	Some SG, red not super prominent
EtOH RPS3	☑	☑	☑	☐	only a few SGs
Ars RACK1	☑	☑	☑	☐	basically all cells SGs
Ars TRAF2	☑	☐	☑	☐	basically all cells SGs
Ars eIF3	☑	☑	☑	☐	basically all cells SGs, faint red
Ars RSP3	☑	☑	☑	☐	basically all cells SGs, nuclei look bigger?
Resv eIF3	☑	☑	☐	☑	faint red
Resv RPS3	☑	☑	☑	☐	some SG
Resv RACK1	☑	☑	☐	☑	
Resv TRAF2	☑	☑	☑	☐	some SG, faint red

Abby

Coverslip	Nuclei Stained	Red Staining	SG Positive	SG Negative	Comments
EtOH RACK1	☑	☑	☐	☑	
EtOH TRAF2	☑	☑	☐	☑	red faint but there
EtOH eIF3	☑	☐	☐	☑	
EtOH RPS3	☑	☑	☑	☐	
Ars RACK1	☑	☑	☑	☐	Lots of SGs
Ars TRAF2	☑	☐	☑	☐	Lots of SGs
Ars eIF3	☑	☑	☑	☐	Lots of SGs
Ars RSP3	☑	☑	☑	☐	
Resv eIF3	☑	☑	☑	☐	
Resv RPS3	☑	☑	☑	☐	
Resv RACK1	☑	☑	☐	☑	
Resv TRAF2	☑	☐	☐	☑	red is too faint

Trends	
Nuclei Stained	Nuclei staining was seen in all the coverslips
Red Staining	Still having issues with staining; EtOH eIF3, Ars TRAF2, Resv TRAF2
SG Staining	All samples stained; lots of SGs seen in ALL Ars samples and some Resv samples

Each researcher examined the staining of the Resveratrol formed SGs and observed problems such as the staining being too faint. The researchers altered the concentrations of the antibody staining to attempt to clear up the imaging to be able to image the slides and overlay to find colocalization.

C. Experiment 1 Trial 2

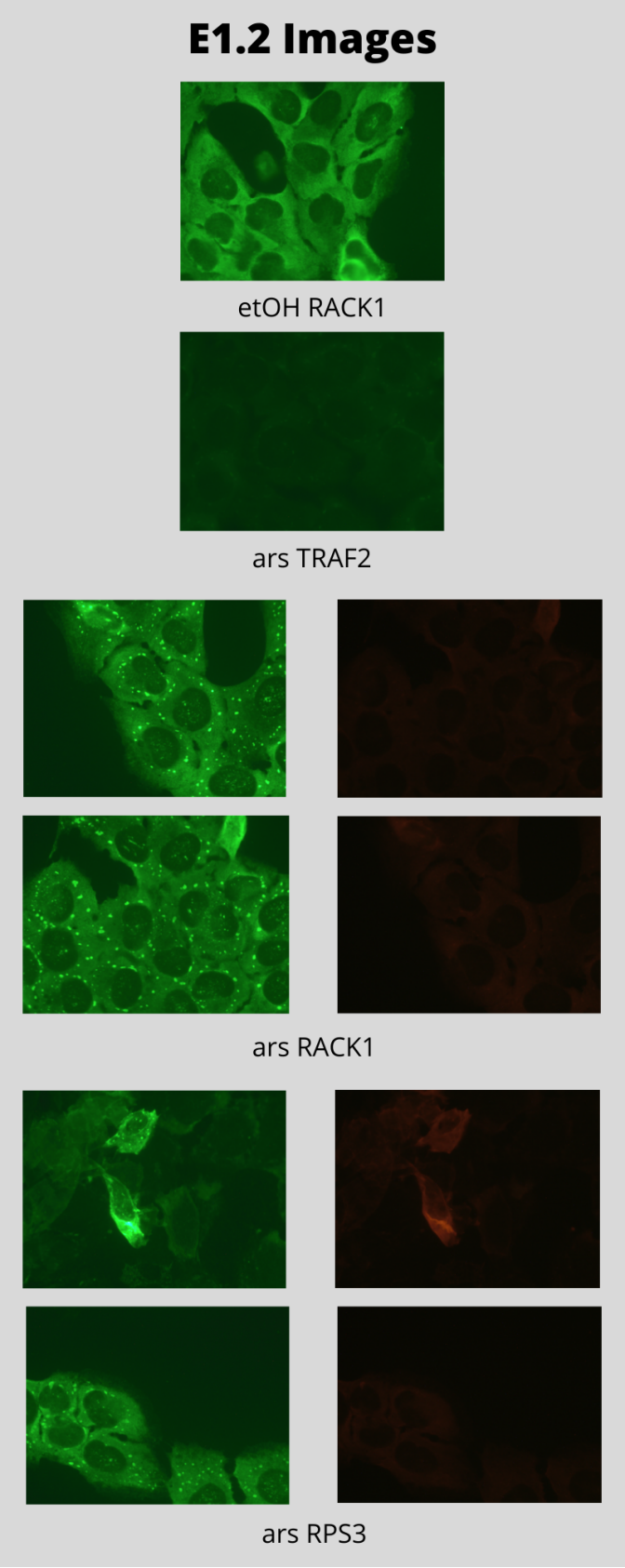

D. Experiment 1 Trial 3

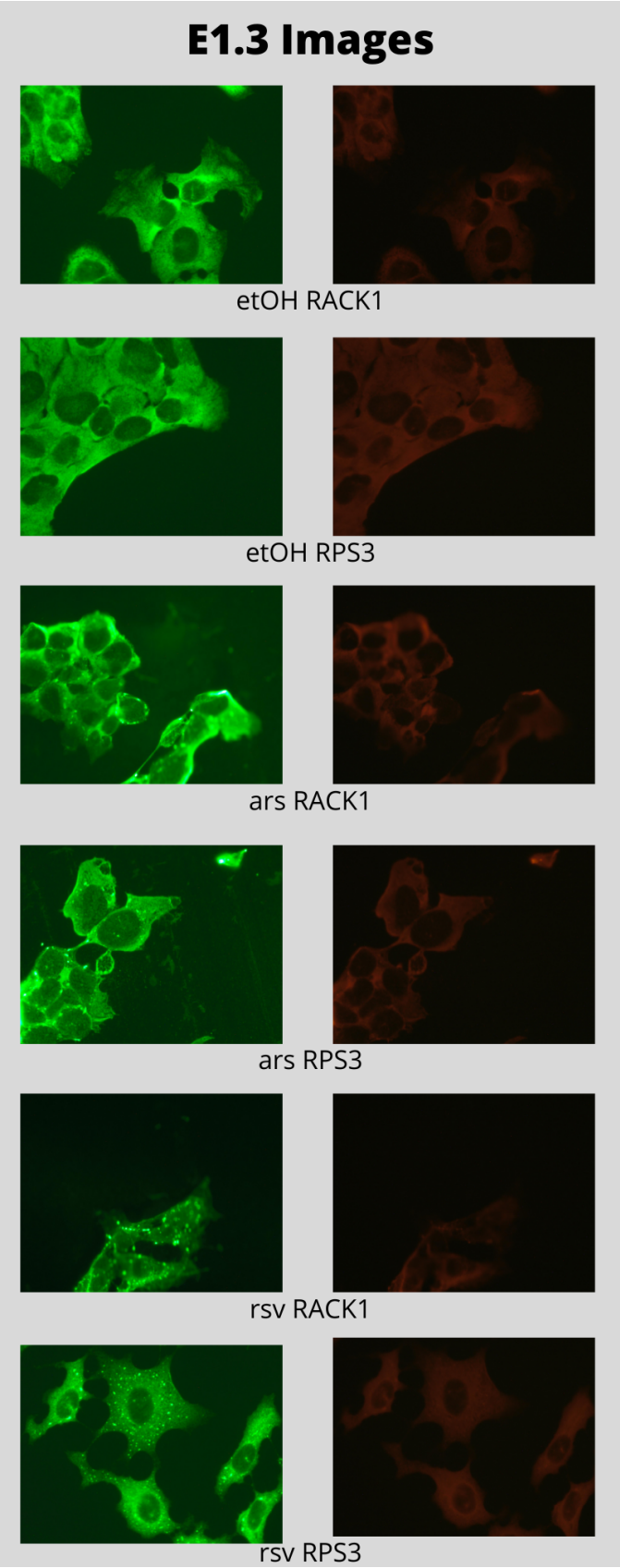

E. Experiment 1 Trial 6 Antibody Staining

Treatment	Antibody	% cells with SGs	Red channel staining
EtOH	TRAF2	0%	stained well
EtOH	eIF3	0%	stained well
EtOH	RACK1	0%	stained well
EtOH	RSP3	0%	stained well
Ars	TRAF2	100%	okay, kinda smudgy, a little blurry
Ars	eIF3	100%	really nice, staining very clear
Ars	RACK1	80%	really nice and clear
Ars	RSP3	80%	okay, kinda smudgy (abby thought was good and really clear)
Rsv	TRAF2	1%	stained pretty, no SG
Rsv	eIF3	1%	stained well but not as defined as Ars samples, little SG seen
Rsv	RACK1	1%	stained very well, no SG
Rsv	RSP3	<1%	stained very well, no SG, kindy smudgy

The red channel staining of each antibody with the three treatments, EtOH, Ars and Rsv, was examined and the qualitative quality of the staining was recorded. The percentage of stress granules present on each slide was also recorded.